Iraqi Journal for Applied Science (IJAS)
Vol. 1, No. 3, December, 2024, pp. 17-24
ISSN: 3006-5828, DOI:10.69923/c5z39695

Synthesis and Characterization of α-Fe_2O_3 NPs and Study Cytotoxicity Against MCF-7 Breast Cancer Cell line

Sazan Ezdeen Maajeed, Abdulqadier Hussien Al khazraji

Department of Chemistry, College of Education for Pure Science
University of Diyala, Diyala, Iraq.

Article Information

Article history:

Received: 15, 07, 2024
Revised: 11, 09, 2024
Accepted: 23, 10, 2024
Published: 30,12, 2024

Keywords:

α-Fe2O3 nanoparticle
chemical precipitation
sol-Gel method
MCF-7 Breast Cancer

Abstract

In this study, iron oxide nanoparticles were synthesized using two different methods: chemical precipitation and the sol-gel method, starting from ferric nitrate (Fe $(NO_3)_3.9H_2O$). Initially, iron hydroxide was obtained from the corresponding salt, followed by calcination at 500°C for five hours to produce the nanoparticles. The synthesized oxides were characterized using various techniques, including TEM and FE-SEM techniques to examine the surface nanoparticles morphology, size and study the microstructures, XRD to analyze the crystalline structures of nanoparticles and EDX to analyze the elemental composition of nanomaterials. The anticancer activity of the synthesized nanoparticles was evaluated against breast cancer cell lines (MCF-7) using MTT assay at concentrations ranging (0 to 320 µg/mL). The results demonstrated that the nanoparticles possess distinctive physical and chemical properties and exhibit anticancer activity. Furthermore, the study found that the preparation method significantly influences the shape, size, and biological effectiveness of the nanoparticles. Hence, the findings highlight the importance of selecting an appropriate preparation method to enhance the desired properties of these particles.

Corresponding Author:

Sazan Ezdeen Maajeed
Department of Computer Science, College of Education for Pure Science
University OF Diyala
Email: sazan.a.majeed.msc23@uodiyala.edu.iq

1. INTRODUCTION

In recent years, there has been a lot of interest in nanotechnology. Nanotechnology is defined as materials ranging in size from 1 to 100 nanometers [1]. Nanomaterials are classified based on their size, but their morphology and geometry also significantly impact their properties. Applications for nanoscale materials are numerous and include electronics, agriculture, and medicine. Through the application of nanotechnology, materials meant for use can be modified by nanoparticles, leading to notable improvements in mechanical, thermal, and barrier properties [2]. The creation of various nanoparticle morphologies, such as particles, spheres, rods, and quantum dot, together offers a wealth of applications and opportunities for technological advancement [3]. Due to their distinctive chemical and physical characteristics, a number of significant nano-oxides, such as manganese sulfate, iron oxide, zinc oxide, magnesium oxide, aluminum oxide, and silver oxide particles, have attracted a lot of attention. They have a wide range of uses in biological applications, such as the treatment of cancer and the healing of wounds, as well as vast applications in oxidation catalysis, sensors, photovoltaic devices, data storage devices, and environmental cleanup [4–7]. Nanotechnology is a promising sign for certain types of cancer disorders, as studies have shown that nanomaterials can eradicate tumors with less damage to vital organs than traditional treatment approaches (radiation therapy and chemotherapy). Several types of inorganic minerals have demonstrated usefulness as active agents in treating malignant tumors [8]. This allows them to work better and provides them with unique physical, chemical, and optical qualities that are required for medical applications like as cancer treatment and detection. Nanoparticles can supplement traditional procedures as well as pioneer new methodologies.

Furthermore, nanoparticles can act as targeting agents, directing them to specific molecular targets within cancer cells, increasing cancer imaging and diagnostic accuracy. Numerous studies have revealed nanoparticles' potential for improving cancer imaging and detection [9-10]. Nanomaterials are methodically manufactured for precise applications in cancer diagnostics and detection, with the goal of developing effective nanomaterials capable of targeting dangerous tumor cells [11]. One of the key challenges in clinical diagnostics is still the early detection of tumors and malignancies. New avenues for cancer imaging, diagnostics, and detection are made possible by the development of sophisticated nanomaterials. Potential uses for metal nanoclusters in cancer diagnosis and treatment have been reported [12-16]. Numerous methods, including chemical ones like the sol-gel process and physical ones like spray pyrolysis and laser ablation, can be used to create nanoparticles. The targeted nanoparticle attributes—size, shape, and composition—determine the technique to be used. Because of this accuracy, nanoparticles with certain characteristics—like stronger magnetic fields or better medication delivery—can be produced. Moreover, nanoparticles can be functionalized to engage in specific chemical or biological interactions. Magnetic-based cancer treatment can benefit from the use of iron oxide nanoparticles, which are known for their biodegradability and distinct deadly mechanisms in their uncoated forms. These nanoparticles use magnetic spin to produce oxygen radicals for cancer detection and treatment. Furthermore, their sensitivity to external electromagnetic fields allows for remote control and localized toxicity caused by reactive oxygen and nitrogen species, reducing negative effects on normal tissues. Furthermore, iron oxide nanoparticles loaded with anti-tumor medicines outperform traditional therapy, as shown in mouse models of breast cancer [17-18].

The breast cancer biomarker miRNA-155, which is recognized for being overexpressed as the cancer progresses, presents difficulties for sensitive detection because of technological constraints. In response, a novel approach for the quick synthesis of magnetic nanoprobes with effective miRNA-155 detection has been established [19]. Long-circulating iron oxide nanoparticles have been shown in another study to aggregate in brain tumors, suggesting that MRI-based tumor detection may benefit from their use. These nanoparticles correlated significantly with tumor cell development in vitro and were particularly localized in tumor cells. They were also taken up by macrophages and endothelial cells in regions of active angiogenesis [20]. This project seeks to synthesis α-Fe2O3 nanoparticles using two methods: chemical precipitation and sol-gel, and examine the attributes of the final product using various physical techniques, as well as cytotoxicity against MCF-7 breast cancer cell line.

2. Materials

Chemicals used were of analytical purity (BDH), including (Fe $(NO_3)_3$. $9H_2O$) with 99% purity, Sodium hydroxide (NaOH), Ethanol, and Deoxygenated distilled water used for synthesizing α-Fe_2O_3 hematite.

2.1 Instruments and Apparatus

The University of Tehran, Iran's College of Science conducted all of the sample analysis. The XRD pattern was obtained using a Siemens model D500 by irradiating the samples with 40 kV at scanning angles ranging from 20° to 80°. A scanning electron microscope (ZEISS model: Sigma VP) was used for surface investigations. TEM (Philips model: CM120) and energy dispersive X-ray spectroscopy (EDX) were used to analyze the elements of α-Fe2O3 nanoparticles.

3. Materials and Methods

3.1 Preparation of α-Fe_2O_3 by Co-precipitation method

Iron oxide α-Fe_2O_3 nanoparticles were synthesized via precipitation: Ferric nitrate nonahydrate (8.2 g) was dissolved in 200 mL deionized water; 0.1 M NaOH added dropwise until pH ≈ 12 Litmus paper was employed to determine the pH measurement, precipitating brown Iron hydroxide (Fe $(OH)_2$). Washed, dried at 80°C for 16 hours to obtain α-Fe_2O_3. Iron oxide synthesis details, including materials and 500°C calcination for 5 hours, were not provided in the initial description and should be clearly distinguished from the α-Fe_2O_3 synthesis.

3.2 Preparation of α-Fe_2O_3 by Sol-Gel method

In 100 milliliters of deionized water, ten grams of ferric nitrate nonahydrate (Fe (NO3)3•9H2O) were dissolved till transparent. Separately, 40 milliliters of deionized water were used to dissolve 6.2 grams of sodium bicarbonate. After the pH of the ferric nitrate solution reached 8, the sodium bicarbonate solution was gradually added while being constantly stirred. This process precipitated brown iron hydroxide. After washing the precipitate with deionized water to remove impurities, it was dried at 100°C and then calcined at 500°C for 5 hours. Calcination at high temperature is essential for converting iron hydroxide into α-Fe2O3 (hematite). The final product obtained after calcination is α-Fe2O3 nanoparticles.

4. RESULTS AND DISCUSSION

The XRD data presented in Figure 1 (a and b) reveals that the creation of α-Fe2O3 nanoparticles is indicated by the 2 theta at 24.28°, 33.3°, 35.82°, 41.07°, 49.7°, 54.24°, 57.75°, and 62.73. The average crystallite size is at 24.37nm and 25.47nmT. he XRD spectra demonstrated that the of α-Fe_2O_3 NPs prepared by chemical preparation is monoclinic phase with cell parameters are a=9.6187 Å b=5.0355 Å c=13.7516 Å β=162.404°crystals, while in the sol-gel method, α-Fe_2O_3 NPs have Trigonal (hexagonal axes) with cell parameters is a=5.0249 Å c=13.7163 Å.

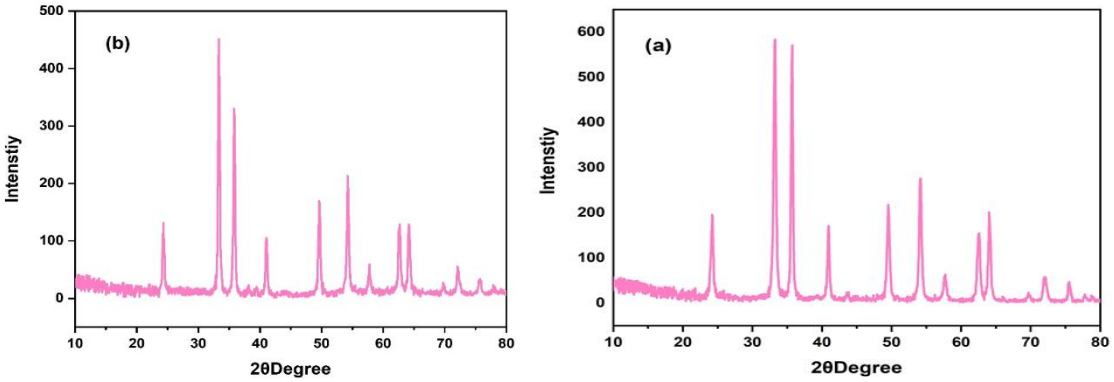

Figure 1: XRD pattern NPs α-Fe2O3 (a) Co-precipitation and (b) sol-gel technique

The α-Fe2O3 nanoparticles that were produced using the co-precipitation and sol-gel techniques, as illustrated in Figures 2 and 3, were found to have spherical, oval, and tubular forms according to the FE-SEM pictures. With an average diameter of 40.97 nm, the spherical nanoparticles are part of the α-Fe2O3 nanoparticles that were generated using the chemical precipitation technique. In contrast, the average diameter of α-Fe2O3 nanoparticles produced using sol gel was 54.35 nm, giving them a nearly oval shape.

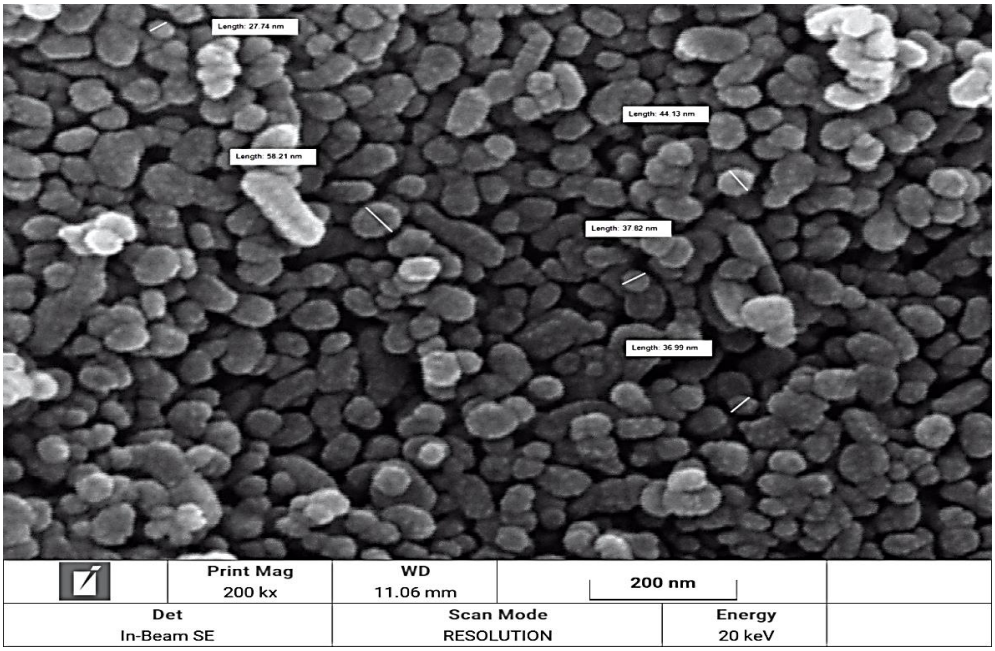

Figure 2: α-Fe2O3 nanoparticles generated using the co-precipitation process captured in a FE-SEM picture.

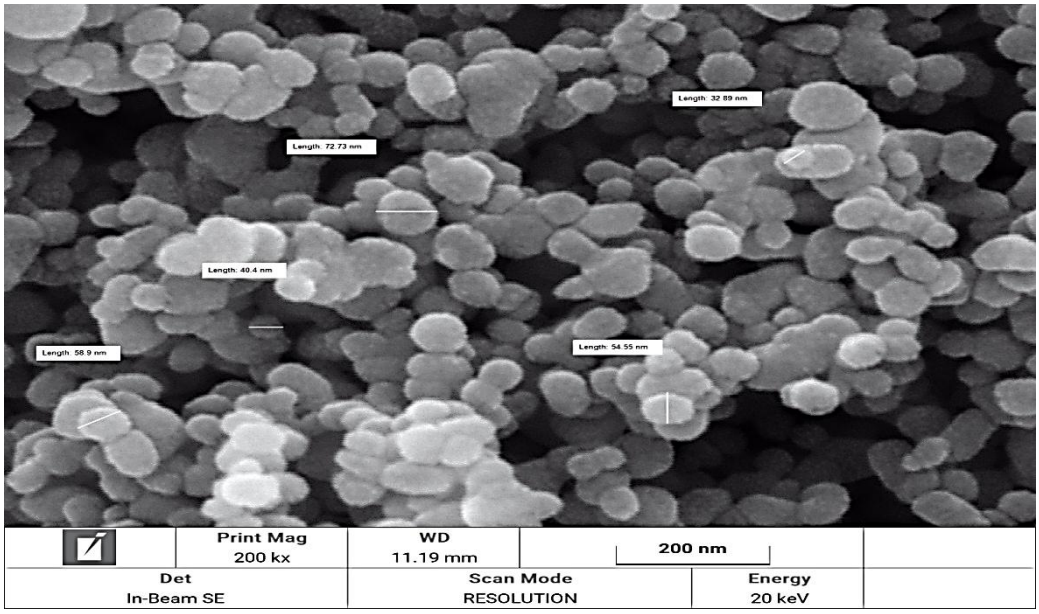

Figure 3: FE-SEM picture of sol-gel-synthesised α-Fe2O3 nanoparticles

Figures 4 and 5, respectively, show the Energy Dispersive X-ray Spectroscopy (EDX) findings of α-Fe2O3 nanoparticles generated using chemical precipitation and Sol-Gel techniques. For the co-precipitation method, the elemental compositions were 80.87% Iron (Fe) and 19.13% oxygen (O). In contrast, the sol-gel method yields a composition of 83.78% Iron (Fe) and 16.22% oxygen (O). These findings confirm the successful formation of α-Fe_2O_3 with good purity.

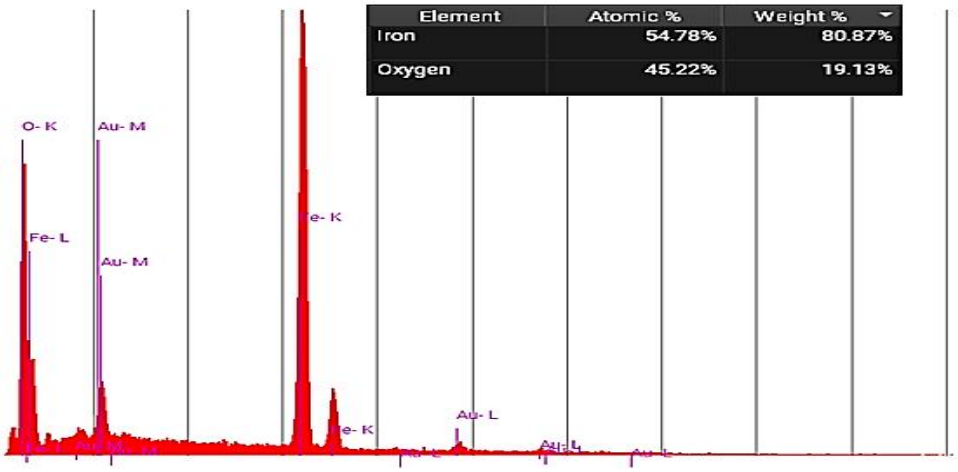

Figure 4: EDX analysis of α-Fe2O3 nanoparticles using the co-precipitation technique is shown in

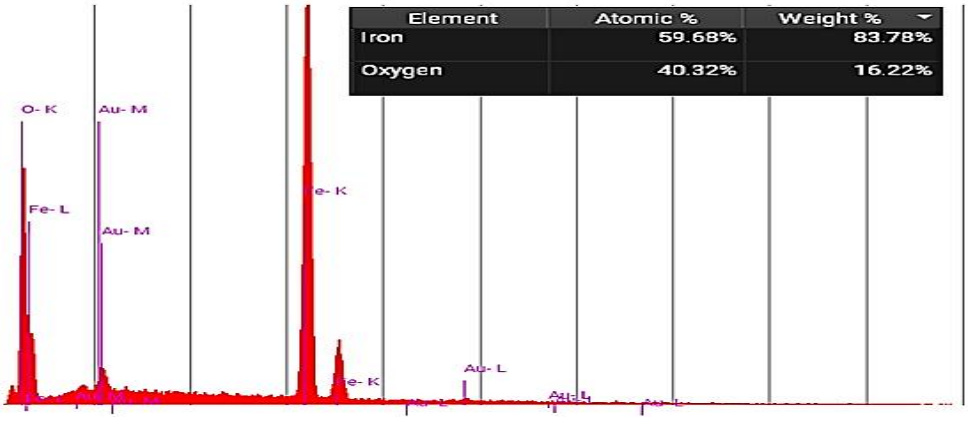

Figure 5: Using the sol-gel technique, EDX analysis of α-Fe2O3 nanoparticles

Figures 6 and 7 shows the transmission electron microscopy (TEM) images at two magnifications (100 and 200 nm) of α-Fe_2O_3 NPs were synthesis by co-precipitation and sol- gel methods respectively. In case of co-precipitation method, the α-Fe_2O_3 NPs appear highly agglomerated with heterogeneous shapes and their sizes range approximately from 14 to 24 nm, while in the sol- gel method the α-Fe_2O_3 NPs were a oval shape with sizes range at 11 to 27 nm.

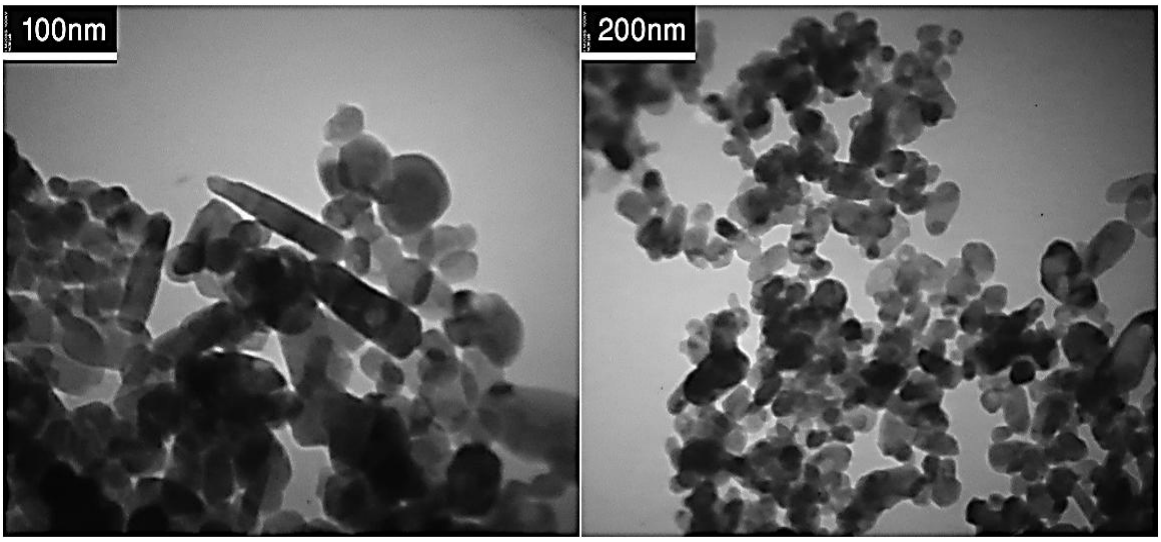

Figure 6. TEM images of α- Fe_2O_3 NPs prepared via chemical precipitation method.

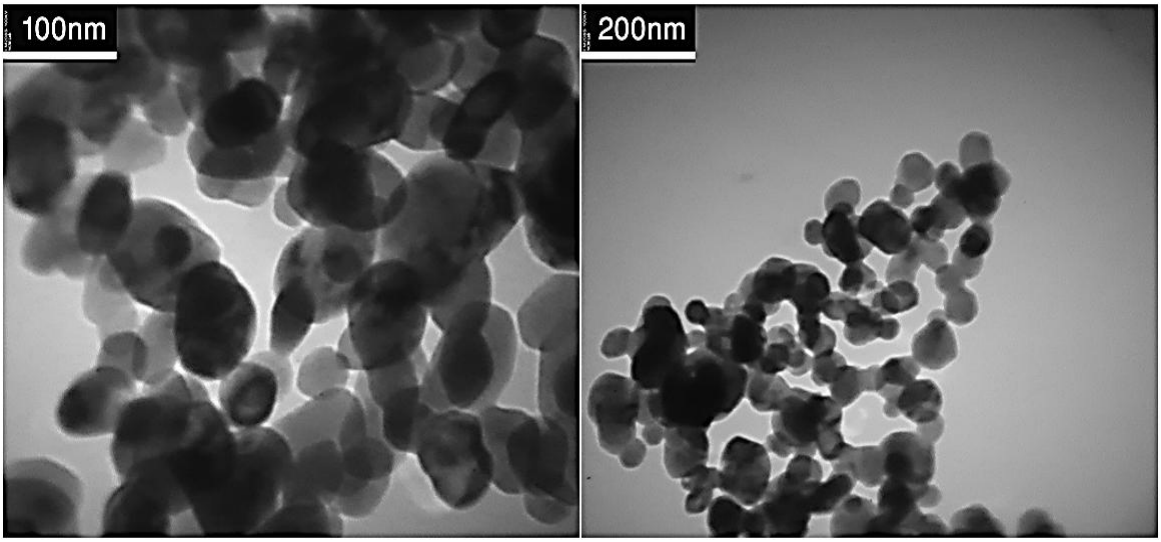

Figure 7. TEM images of α- Fe_2O_3 NPs prepared via sol-gel method.

4.1 Cytotoxicity of α-Fe_2O_3 NPs against MCF-7 Breast Cancer Cell line

The purpose of this study was to examine how α-Fe2O3 nanoparticles affected MCF-7 breast cancer cells. After exposing the cells to different α-Fe2O3 concentrations (320, 160, 80, 40, and 20 µg/mL) for a whole day, the MTT test was used to assess the viability of the cells. The results showed that as α-Fe2O3 concentrations in MCF-7 cells increased, there was a dose-dependent rise in cell mortality. Figures 8 and 9, together with Tables 1 and 2, show the outcomes for α-Fe2O3 produced by the sol-gel technique and chemical precipitation. It was found that the α-Fe2O3 nanoparticles had an IC50 value of 113.4 µg/mL.

4.2 Method of Testing

The cytotoxicity of synthesized metal oxide nanoparticles was assessed against breast cancer cell lines using the MTT assay. Cells were cultured in RPMI 1640 medium and incubated at 37°C with 5% CO_2 for 5 days, with daily monitoring using an inverted microscope. Nanoparticle solutions were prepared by dispersing 5 mg of each oxide in 50 µL of DMSO, then diluting to obtain concentrations of 20, 40, 80, 160, and 320 µg/mL. MTT solution was made by dissolving 5 mg of the dye in 1 mL of PBS, filtered, and stored in a dark bottle at 4°C. 100 µL of cell suspension at 1x10^4 cells/mL was added to each well of a microplate and incubated for 24 hours at 37°C with 5% CO_2. After incubation, 100 µL of nanoparticle oxide solutions were added to achieve final concentrations (320, 160, 80, 40, 20 µg/mL), with three replicates per concentration, and the plates were incubated under the same conditions for an additional 24 hours.

Following this, 10 µL of MTT solution was added to each well, and the plate was incubated for 5 hours under the same conditions. The color change in each well was measured using a microplate reader at 570 nm. The first control consisted of cells only, while the second control included cells with DMSO. Cell growth inhibition was calculated using the following equation.

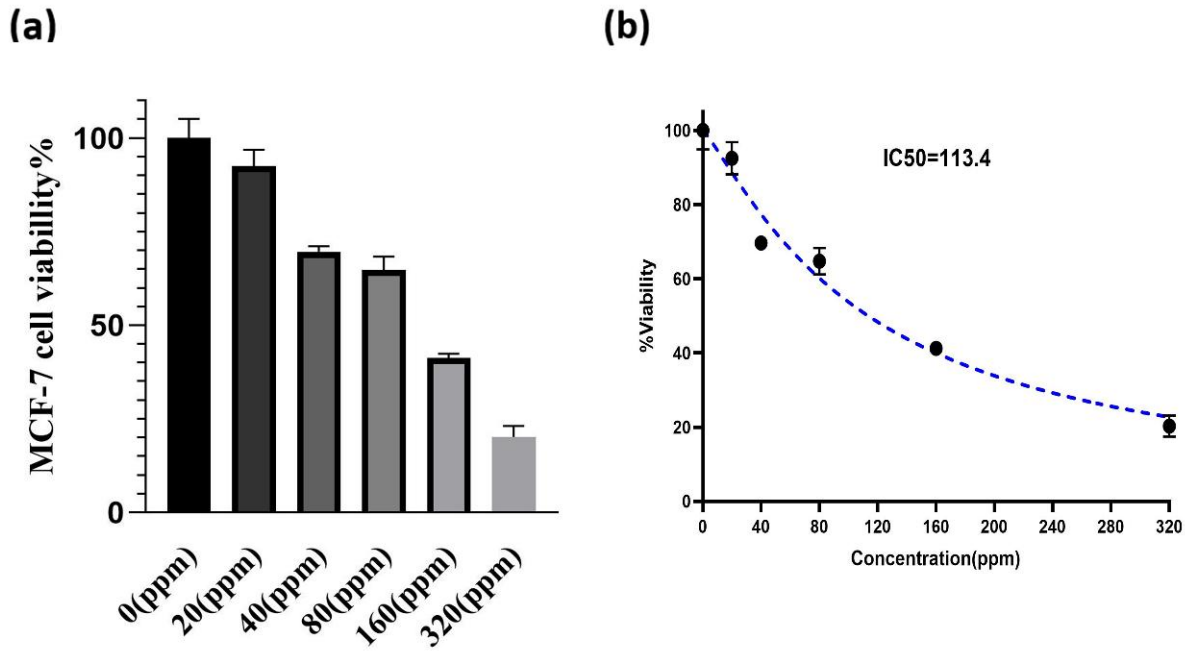

Figure 8: (a) Illustrates the percentage of cancer cell killing, (b) shows the IC50 α-Fe_2O_3 NPsprepared using chemical precipitation method.

Table (1). showing concentrations, killing percentage, and cell viability of cancer cells by α-Fe_2O_3 NPs prepared using chemical precipitation method.

α-Fe_2O_3 concentration (µg/mL)	Cell Death (%)	Cell Viability (%)
20	7.5163	92.4837
40	30.3471	69.6529
80	35.2713	64.7287
160	58.7684	41.2316
320	79.765	20.235

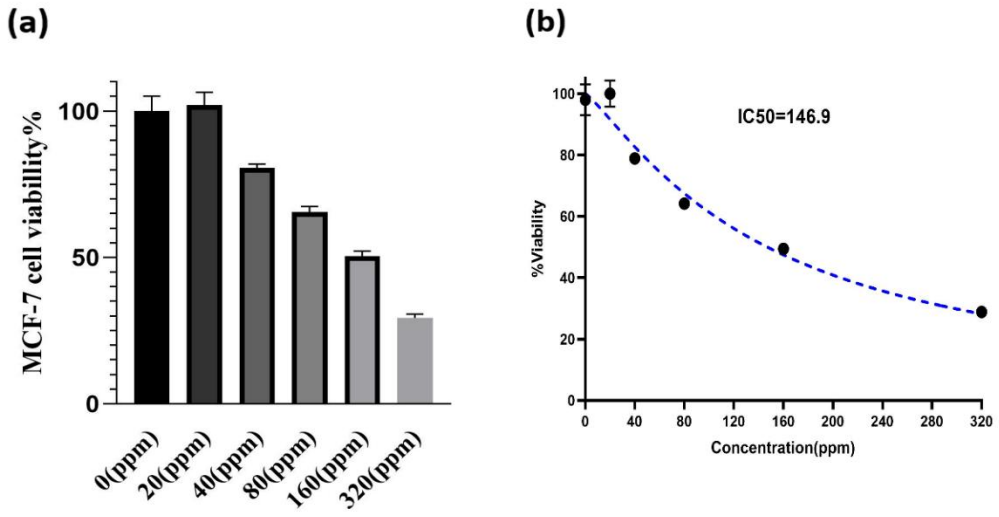

Figure 9: (a) Illustrates the percentage of cancer cell killing, (b) shows the IC50 α-Fe_2O_3 NPs prepared using sol-gel method.

Table (2): Concentrations, killing percentage, and cell viability of cancer cells by α-Fe_2O_3 NPs prepared using sol-gel method.

α-Fe_2O_3 concentration (µg/mL)	Cell Death (%)	Cell Viability (%)
20	2.039	97.961
40	19.473	80.527
80	34.50	65.50
160	49.579	50.421
320	70.57	29.43

These results indicate that iron induces dose-dependent cytotoxic effects on MCF-7 cells. Highlighting its potential as a therapeutic agent for breast cancer treatment. Further investigations into the underlying mechanisms and in vivo studies are warranted to fully elucidate its therapeutic efficacy and safety profile. IC50 represents the concentration at which cell growth is inhibited by 50%, underscoring the potent inhibitory effect of α-Fe_2O_3 on MCF-7 cell proliferation. These findings suggest that α-Fe_2O_3 holds promise as a candidate for further studies as an inhibitor of breast cancer cell growth, highlighting the importance of exploring its mechanisms of action in cancer cells

5. CONCLUSION

In this study, two procedures (chemical precipitation and sol-gel) were successfully used to manufacture the α-Fe2O3 NPs utilizing Fe (NO3)3. 9H2O) as precursors. The presence of α-Fe2O3 NPs was verified using many methods (XRD, TEM and FE-SEM, EDX). The α-Fe2O3 NPs phase, which was a monoclinic phase of iron oxide synthesized by chemical precipitation technique and trigonal (hexagonal axis) in the case of the sol-gel method, was shown by the XRD spectra to be affected by the kind of method utilized. The α-Fe2O3 nanoparticles produced using the chemical precipitation technique have spherical nanoparticles with an average diameter of 40.97 nm. On the other hand, the α-Fe2O3 nanoparticles produced through sol gel exhibit almost oval shapes with average diameters of 54.35 nm, as demonstrated by FE-SEM pictures. The presence of oxygen and iron in the α-Fe2O3 NPs made using the two procedures was verified by EDX spectra. The influence of type procedure on the size and form of produced α-Fe2O3 NPs was clearly seen in TEM pictures. The findings show that α-Fe2O3 exhibited dose-dependent anticancer properties against human breast cancer cell lines.

ACKNOWLEDGEMENTS
The authors appreciate the College of Education for Pure Sciences - University of Diyala - for using laboratories with the necessary equipment to carry out the experiment.

REFERENCES

[1] Y. H. Yap, A. A. Azmi, N. K. Mohd, F. S. J. Yong, S. Y. Kan, M. Z. A. Thirmizir, and P. W. Chia, "Green synthesis of silver nanoparticle using water extract of onion peel and application in the acetylation reaction," *Arabian Journal for Science and Engineering*, vol. 45, pp. 4797-4807, 2020.

[2] M. Costello-Caulkins, "Nanotechnology Patent Law: A Case Study of United States and European Patent Applications," *Santa Clara High Tech. LJ*, vol. 37, p. 337, 2021.

[3] C. P. Devatha and A. K. Thalla, "Green synthesis of nanomaterials," in *Synthesis of inorganic nanomaterials*, Woodhead Publishing, 2018, pp. 169-184.

[4] S. Torabi, M. J. K. Mansoorkhani, A. Majedi, and S. Motevalli, "Synthesis, medical and photocatalyst applications of nano-Ag2O," *Journal of Coordination Chemistry*, vol. 73, no. 13, pp. 1861-1880, 2020.

[5] K. Huang, C. Li, Y. Zheng, L. Wang, W. Wang, and X. Meng, "Recent advances on silver-based photocatalysis: Photocorrosion inhibition, visible-light responsivity enhancement, and charges separation acceleration," *Separation and Purification Technology*, vol. 283, p. 120194, 2022.

[6] F. A. Kiani, U. Shamraiz, and A. Badshah, "Enhanced photo catalytic activity of Ag2O nanostructures through strontium doping," *Materials Research Express*, vol. 7, no. 1, p. 015035, 2020.

[7] A. J. Al-Sarray, I. M. H. Al-Mousawi, and T. H. Al-Noor, "Acid Activation of Iraqi Bentonite Clay: Its Structural, Dielectric and Electrical Behavior at Various Temperatures," *Chemical Methodologies*, vol. 6, no. 4, pp. 331-338, 2022.

[8] R. Qiu, D. Zhang, Y. Mo, L. Song, E. Brewer, X. Huang, and Y. Xiong, "Photocatalytic activity of polymer-modified ZnO under visible light irradiation," *Journal of Hazardous Materials*, vol. 156, no. 1-3, pp. 80-85, 2008.

[9] S. Swain, P. Kumar Sahu, S. Beg, and M. S. Manohar Babu, "Nanoparticles for cancer targeting: current and future directions," *Current Drug Delivery*, vol. 13, no. 8, pp. 1290-1302, 2016.

[10] W. Zhang, Y. Lu, Y. Zang, J. Han, Q. Xiong, and J. Xiong, "Photodynamic therapy and multi-modality imaging of up-conversion nanomaterial doped with AuNPs," *International Journal of Molecular Sciences*, vol. 23, no. 3, p. 1227, 2022.

[11] A. Abed, M. Derakhshan, M. Karimi, M. Shirazinia, M. Mahjoubin-Tehran, M. Homayonfal, M. R. Hamblin, S. A. Mirzaei, H. Soleimanpour, S. Dehghani, and F. F. Dehkordi, "Platinum nanoparticles in biomedicine: Preparation, anti-cancer activity, and drug delivery vehicles," *Frontiers in Pharmacology*, vol. 13, p. 797804, 2022.

[12] A. Ramanathan, "Toxicity of nanoparticles: challenges and opportunities," *Applied Microscopy*, vol. 49, no. 1, p. 2, 2019.

[13] P. Patel, V. Patel, and P. M. Patel, "Synthetic strategy of dendrimers: A review," *Journal of the Indian Chemical Society*, vol. 99, no. 7, p. 100514, 2022.

[14] X. Wang, J. Li, W. Zhang, P. Li, W. Zhang, H. Wang, and B. Tang, "Evaluating diabetic ketoacidosis via a MOF sensor for fluorescence imaging of phosphate and pH," *Chemical Communications*, vol. 58, no. 18, pp. 3023-3026, 2022.

[15] W. Zhang, X. Wang, P. Li, W. Zhang, H. Wang, and B. Tang, "Evaluating hyperthyroidism-induced liver injury based on in situ fluorescence imaging of glutathione and phosphate via nano-MOFs sensor," *Analytical Chemistry*, vol. 92, no. 13, pp. 8952-8958, 2020.

[16] L. Gao, Y. Zhang, L. Zhao, W. Niu, Y. Tang, F. Gao, P. Cai, Q. Yuan, X. Wang, H. Jiang, and X. Gao, "An artificial metalloenzyme for catalytic cancer-specific DNA cleavage and operando imaging," *Science Advances*, vol. 6, no. 29, p. eabb1421, 2020.

[17] D. Chakraborty, T. S. Viveka, K. Arvind, V. Shyamsundar, M. Kanchan, S. A. Alex, N. Chandrasekaran, R. Vijayalakshmi, and A. Mukherjee, "A facile gold nanoparticle–based ELISA system for detection of osteopontin in saliva: Towards oral cancer diagnostics," *Clinica Chimica Acta*, vol. 477, pp. 166-172, 2018.

[18] Y. Zeng, J. Bao, Y. Zhao, D. Huo, M. Chen, M. Yang, H. Fa, and C. Hou, "A sensitive label-free electrochemical immunosensor for detection of cytokeratin 19 fragment antigen 21-1 based on 3D graphene with gold nanoparticle modified electrode," *Talanta*, vol. 178, pp. 122-128, 2018.

[19] M. Sharma, "Transdermal and intravenous nano drug delivery systems: present and future," in *Applications of Targeted Nano Drugs and Delivery Systems*, Elsevier, 2019, pp. 499-550.

[20] U. Shanker, M. Rani, and C. M. Hussain, Eds., *Green Functionalized Nanomaterials for Environmental Applications*. Elsevier, 2021.

BIOGRAPHIES OF AUTHORS

Sazan Ezdeen Maajeed

General specialization: Chemistry specialization: Physical Chemistry, Master's degree from Diyala University - College of Education for Pure Sciences - Department of Chemistry, fluent in Arabic, Kurdish and English. And possessed skills in nanomaterials diagnostic devices and computer programs.

Email: sazan.a.majeed.msc23@uodiyala.edu.iq

Abdulqadier Hussien Al khazraji

General specialization: Chemistry Specialization: Physical Chemistry, Holder of a PhD from Moscow Technological University - Russian Federation, Position: Assistant Dean for Administrative Affairs, Research field: Nano Research, Email: abdulqadier.niama@uodiyala.edu.iq